ID: 1123

Experimental Evidence of Nonlinear Avalanche Dynamics of Energetic Particle Modes

L.M. Yu[1], F. Zonca[2,3], Z.Y. Qiu[3], L. Chen[3], W. Chen[1], X.T. Ding[1], X.Q. Ji[1], T. Wang[4], T.B. Wang[1], R.R. Ma[1], B.S. Yuan[1], P.W. Shi[5], Y.G. Li[1], L. Liu[1], Z.B. Shi[1], J.Y. Cao[1], J.Q. Dong1, M. Xu[1] and X.R. Duan[1]

[1]Southwestern Institute of Physics, Chengdu, China
[2]Center for Nonlinear Plasma Science and ENEA C. R. Frascati, Frascati (Roma), Italy
[3]Institute for Fusion Theory and Simulation, Zhejiang University, Hangzhou, China
[4]Shenzhen University, Shenzhen, China
[5]Dalian University of Technology, Dalian, China

Email: yulm@swip.ac.cn

ABSTRACT

Experimental observations in HL-2A tokamak give new experimental evidences of energetic particle mode (EPM) avalanche:

- In a strong EPM burst, the mode structure propagates radially outward, while the frequency of the dominant mode changes self-consistently to maximize wave-particle power exchange and mode growth.
- This suggests that significant energetic particle transport occurs in this avalanche phase, in agreement with theoretical framework of EPM convective amplification.
- A simplified Relay Runner Model (F. Zonca) yields satisfactory interpretations of the measurements.

BACKGROUND

- The energetic particles (EPs), with sufficiently strong pressure gradient, can excite EPMs [1-4], which emerges as discrete fluctuation out of the shear Alfvén continuum at the frequency for maximal wave-EP power exchange above the threshold condition due to continuum damping. The critical level of tolerable EP losses in a fusion device can be more severe in the presence of EPM.
- The early nonlinear theories [5-7] have expected the role of the EPs radial displacements on the time evolution of a strongly driven mode as the EPM.
- If the EPs move outward, they can locally alter the EP gradient and destabilize a new wave that transports them further, where a new wave is destabilized, much like different runners do in a relay race. The model for the nonlinear evolution is named relay runner model (RRM) [6].
- The expected self-consistent nonlinear evolution of the EPM and the EPs have not been unambiguously observed in experiments up to now.

[1] L. Chen, Phys. Plasmas 1, 1519 (1994); [2] F. Zonca et al., Plasma Phys. Control. Fusion 48, 537 (2006); [3] L. Chen and F. Zonca, Review of Mordern Physics 88, 015008 (2016); [4] W.W. Heidbrink, Phys. Plasma 15, 055501 (2008); [5] R.B. White et al., Phys. Plasmas 26, 2958 (1983); [6] F. Zonca and L. Chen, 6th IAEA TCM on Energetic Particles in Magnetic Confinement Systems, Oct. 12-14, 1999, JAERI, Naka, JAPAN; [7] L. Chen and F.Zonca, Nucl. Fusion 47, S727 (2007).

EXPERIMENTAL RESULTS

HL-2A Tokamak & NBI System

HL-2A tokamak:

- R_0=1.65 m, a=0.4 m
- I_p=100-450 kA
- B_t=1.0-2.5 T
- n_e=(0.2-5.5)$\times 10^{19}$ m^{-3}
- Divertor & limiter

NBI system:

- 2 co-injected beam lines
- Injection angle: 58.1^0 (as shown in Fig.1)
- Maximum injection power: P_{NBI}=1.5 MW
- E_h=38-45 keV

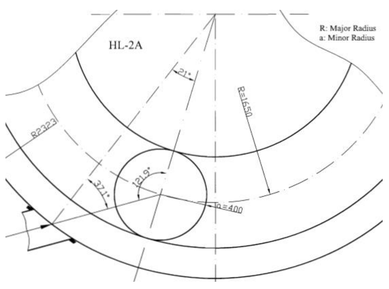

Fig.1 Injection direction and path of NBI

Poloidal Mirnov Probes & Soft X-ray (SXR) Arrays

- The Alfvénic instabilities can be detected by from the spectrogram of Mirnov probes and SXR arrays;
- The poloidal/toroidal mode numbers (m/n) of the wave care measured by the phase shift method by Mirnov probe arrays;
- The structure and evolution of the modes inside r=0.33 m radius cross section can be obtained by tomography technology of SXR arrays.

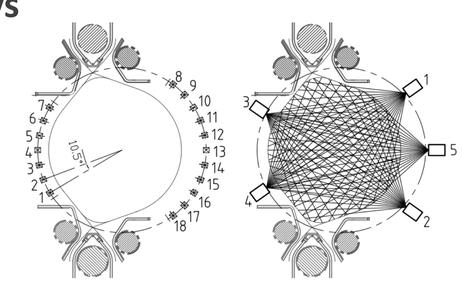

Fig.2 Arrangements of poloidal Mirnov probes (left) and SXR arrays (right) on HL-2A

Poloidal Mirnov Probes: 18 poloidal Mirnov probes, 7 Mirnov probes localized in the high-field side and 11 localized in the low-field side, and the interval angle is Δθ= 10.5^0 between each of the two adjacent channels, as shown in Fig.2 (left);
Toroidal Mirnov Probes: 10 toloidal Mirnov probes localized low field side;
Soft X-ray arrays: 5 sets of SXR detection systems, each set consisting 20 evenly distributed arrays, as shown in Fig.2 (right).

EPMs on HL-2A

Strong EPMs are found in NBI heating plasmas in shot I, as shown in Fig.3.

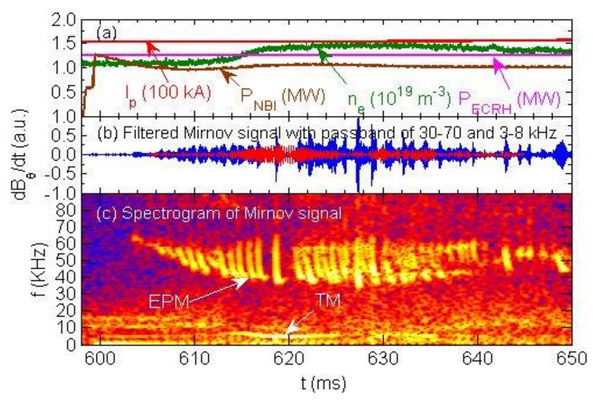

Fig.3 EPMs observed in NBI heating plasmas on HL-2A in shot I.

- Discharge parameters in shot I:
  I_p~155 kA, n_e~(1.1-1.5)$\times 10^{19}$ m^{-3},
  B_t=1.38 T, P_{NBI}=1.0 MW, E_b~42 keV
- Strong EPMs appear during NBI heating;
- Frequency chirping down rapidly from 65 to 35 kHz within 1 ms (Δf=30 kHz, $\Delta f/f$~50%).

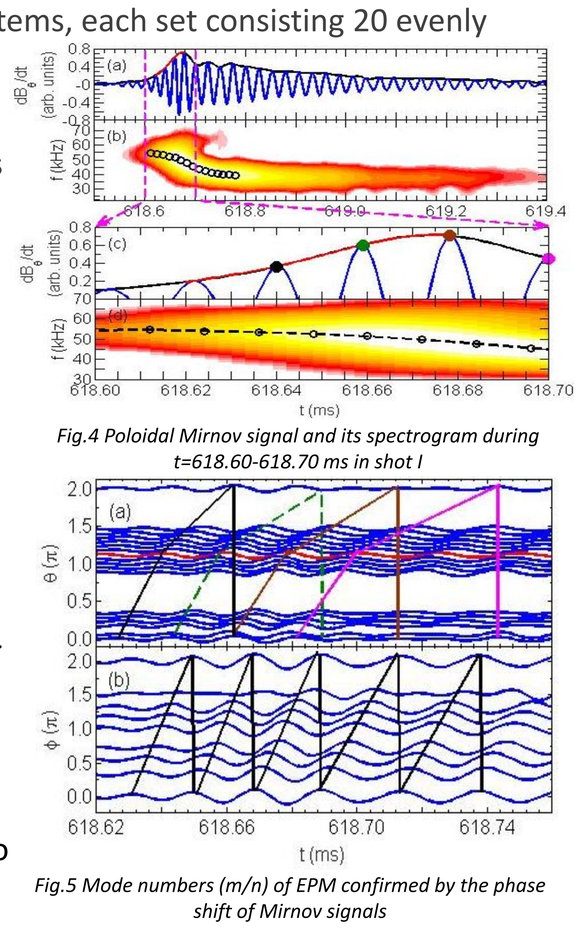

Fig.4 Poloidal Mirnov signal and its spectrogram during t=618.60-618.70 ms in shot I

Fig.5 Mode numbers (m/n) of EPM confirmed by the phase shift of Mirnov signals

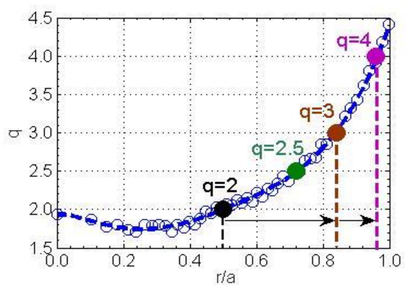

Fig.6 q-profile near t=618 ms and the rational surface of q=2, 2.5, 3 and 4 labeled by the black, green, brown and purple circles respectively.

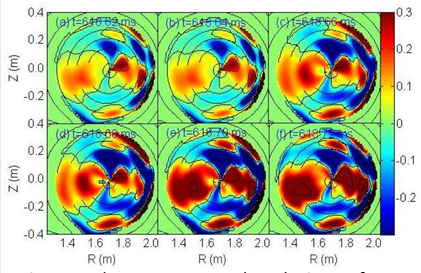

Fig.7 Mode structures and evolutions of EPM in poloidal cross section inside r=0.33 m region obtained by tomography of SXR arrays.

In a strong burst — a successive frequency chirping down process during t=618.64-618.70 ms in shot I (Fig.4):

- Frequency of EPM sweeps down from 55 to 43 kHz;
- The poloidal mode number changes from m=2 to 3, and then from 3 to 4, while the toroidal mode number keeps n=1 all the time, as shown in Fig.5;
- It is indicated that: (1) The mode propagate radially from the core (q=m/n=2) to the edge (q=3 and 4), as shown in Fig.6. (2) Energetic ions are exciting the EPM all the time in the outward path of being expelled;
- Radial velocity of the mode (V_p):

$$V_p = \frac{\Delta r}{\Delta t} = \frac{0.36 - 0.19}{618.70 - 618.64} = 2.83\ \mathrm{km/s}$$

Radial propagation of EPM can also be proved by tomography technology of SXR:

- m=2 element are dominant firstly, then the mode propagates outward. At last, m=4 elements are dominant as shown in Fig.7.

Theory Analysis and Verification

Owning to the injection angle of NBI, EPM is driven by the transit resonance of the predominantly circulating EP population, i.e.,

$$\omega = \omega_{tr} \equiv \frac{\sqrt{2(E/mi - \mu B)}}{qR_0} \qquad (1)$$

with E and m_i being the energy and mass of ions, and $\mu \equiv v_\perp^2/(2B)$.

EP transit frequency changing rate due to EP energy change and radial transport,

$$\dot{\omega} = \dot{\omega}_{tr} \simeq \frac{\partial \omega_{tr}}{\partial E}\dot{E} + \frac{\partial \omega_{tr}}{\partial r}\dot{r} \qquad (2)$$

For HL-2A parameters, the chirping rate contribution due to radial transport is much smaller than that due to energy change. For a single-n coherent fluctuation of interest here, one obtains $\dot{E} \simeq (\omega/n)\dot{P}_\phi$ from the conservation of extended phase space Hamiltonian, with P_ϕ being the toroidal angular momentum and $\dot{P}_\phi \simeq -m_i\Omega_i r\dot{r}/q$.

$$\dot{\omega} = \dot{\omega}_{tr} \simeq -\frac{\Omega_i r}{nR_0^2 q^3}\dot{r} \qquad (3)$$

q	$t\ (ms)$	$A\ (a.u.)$	$r\ (m)$	$f\ (kHz)$	$\dot{\omega}\ (10^9\ rad/s^2)$	$\dot{r}\ (km/s)$
2	618.64	0.36	0.19	53.10	−0.42	0.78
2.5	618.66	0.61	0.27	51.27	−0.76	1.93
3	618.68	0.71	0.31	48.62	−1.06	4.00

- Radial velocity at q=2, 2.5 and 3 rational surfaces and the corresponding experimental data are shown in Table.1;
- The averaged radial velocity of EPs ($\bar{\dot{r}}$) is about 2.23 km/s;
- Compare to above result, $|\dot{r}/V_p| \approx O(1)$, i.e., the observed mode radial propagation velocity is comparable to that of EPs, as predicted by RRM model.

The instantaneous radial velocity of the outward pumped EPs ($\dot{r}$) can be derived from equation (3) as

$$\dot{r} = -\frac{nR_0^2 q^3}{(\Omega_i r)}\dot{\omega} \qquad (4)$$

On the other hand, the radial velocity of resonant EPs can be derived as

$$\dot{r} = \frac{c}{B_0}\hat{\boldsymbol{r}}\cdot\hat{\boldsymbol{b}}\times\delta\boldsymbol{E}_{\boldsymbol{\theta}} \simeq \frac{k_\theta}{B_0 k_\parallel k_r}A \qquad (5)$$

Here, k is the WKB wavenumber, $\delta\boldsymbol{E}_{\boldsymbol{\theta}}$ is the poloidal electric field perturbation, and A is the time derivative of the perturbed poloidal magnetic field from Mirnov signal, i.e., $A = \partial_t \delta B_\theta$.

Substituting into equation (3), noting that $k_\theta \equiv nq/r$ and $k_\parallel \equiv (nq - m)/(qR_0)$, one obtains

$$\dot{\omega} \simeq -\frac{\Omega_i}{q^2 R_0^2 B_0 k_\parallel k_r}A \propto \frac{1}{q^{1+\alpha}}A \qquad (6)$$

with $|\alpha| \le 1$ and $q^{-\alpha}$ accounting for the radial dependence of nq-m and k_r.

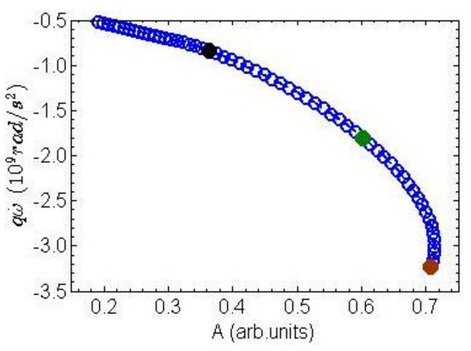

Fig.8 Relationship between mode amplitudes A and $q\dot{\omega}$ in experiment.

- The scaling $A \propto q\dot{\omega}$ can be proved by experimental results, as shown in Fig. 8.

CONCLUSION

The experimental evidence of nonlinear avalanche dynamics of the EPM is found in NBI heating plasma on HL-2A.

- The m changes from 2 to 4 successively, while n always keeps constant as 1, indicating that the EPM propagates from the core to edge of plasmas gradually. The tomography of SXR arrays also illuminates the fast nonlinear avalanche;
- The product of $\dot{\omega}$ and q factor is proportional to A in the nonlinear avalanche processes, e.g., $A \propto q\dot{\omega}$, which is consistent with the nonlinear RRM model prediction;
- The estimated radial velocity of the resonant EPs is close to the radial propagating velocity of the EPM in experiment, confirming the convective amplification mechanism underlying EPM self-consistent nonlinear dynamics;
- Experimental evidence also supports the non-adiabatic nature of the EPM nonlinear dynamics connected with continuous trapping and de-trapping of EPs and their convective transport;
- This is the first time that experimental evidence of EP nonlinear avalanche dynamics, is demonstrated, consistent with theoretical predictions, which is of crucial importance for the understanding of transport and redistribution of EPs in future fusion reactor, such as ITER.